

RESEARCH

Open Access



Simplified Effective Compressive Strengths of Columns with Intervening Floor Slabs

Seung-Ho Choi¹, Jin-Ha Hwang², Sun-Jin Han¹, Hae-Chang Cho³, Jae Hyun Kim¹ and Kang Su Kim^{1*}

Abstract

The current design codes discuss the effective compressive strengths of columns, which reflect a decrease in load transfer performance that can occur when columns and slabs have different concrete compressive strengths. The effective compressive strength of a column increases as it is confined by the slab, and the design codes mandate three different effective compressive strengths for interior columns (confinement on four sides), exterior columns (confinement on three sides), and corner columns (confinement on two sides). For both corner and exterior columns, the confinement effect of the slab is significantly smaller than that for the interior column, and there is a more marked decrease in load transfer performance. However, there is still a lack of theoretical studies investigating the effective compressive strengths of the corner and exterior columns. Therefore, based on the analysis model established in previous research, this study has proposed an equation for calculating the effective compressive strengths of the corner, exterior and isolated columns without any confinement effects of the slab. In addition, axial loading tests of isolated columns were conducted and the proposed equation was verified.

Keywords: effective compressive strength, normal strength concrete, high strength concrete, slab, column, reinforced concrete

1 Introduction

High strength concrete (HSC), which has a compressive strength greater than 50 MPa, has been increasingly used in a number of applications, and reducing the cross-section of the column has been shown to lead to a more efficient use of floor space (Lee and Mendis 2004). By contrast, since increasing the compressive strength of slab concrete does not significantly contribute to enhancing flexural performance, normal strength concrete (NSC) is typically used for slabs (Gamble and Klinar 1991). When HSC is used for columns and NSC is used for slabs, the placement of NSC between the upper and lower HSC columns affects the load transfer mechanism of the columns.

The current design codes (ACI 318-19; CSA A23.3-14 (2019)) include a provision that requires that the column can ensure proper load transfer performance when the upper/lower columns and slabs have different compressive strengths, as shown in Fig. 1 (Urban and Gołdyn 2015). The ACI 318-19 suggests that if the compressive strength of the column concrete exceeds 1.4 times the compressive strength of the slab concrete, the column concrete should either be extended beyond the column face by a distance greater than 600 mm as shown in Fig. 1b, be reinforced with a vertical dowels or spirals as shown in Fig. 1c, or adopt the effective compressive strength (f'_{ce}). Here, when four sides of the column are confined by the slab (hereinafter referred to as an interior column), the effective compressive strength is assumed to be the strength of the concrete, consisting of the sum of 75% of the column concrete strength (f'_{cc}) and 35% of the slab concrete strength (f'_{cj}). In addition, if two sides of the column are confined (hereinafter referred to as a corner column) or three sides of the column are confined

*Correspondence: kangkim@uos.ac.kr

¹ Department of Architectural Engineering, University of Seoul, 163 Siripdaero, Dongdaemun-gu, Seoul 02504, Republic of Korea
Full list of author information is available at the end of the article
Journal information: ISSN 1976-0485 / eISSN 2234-1315

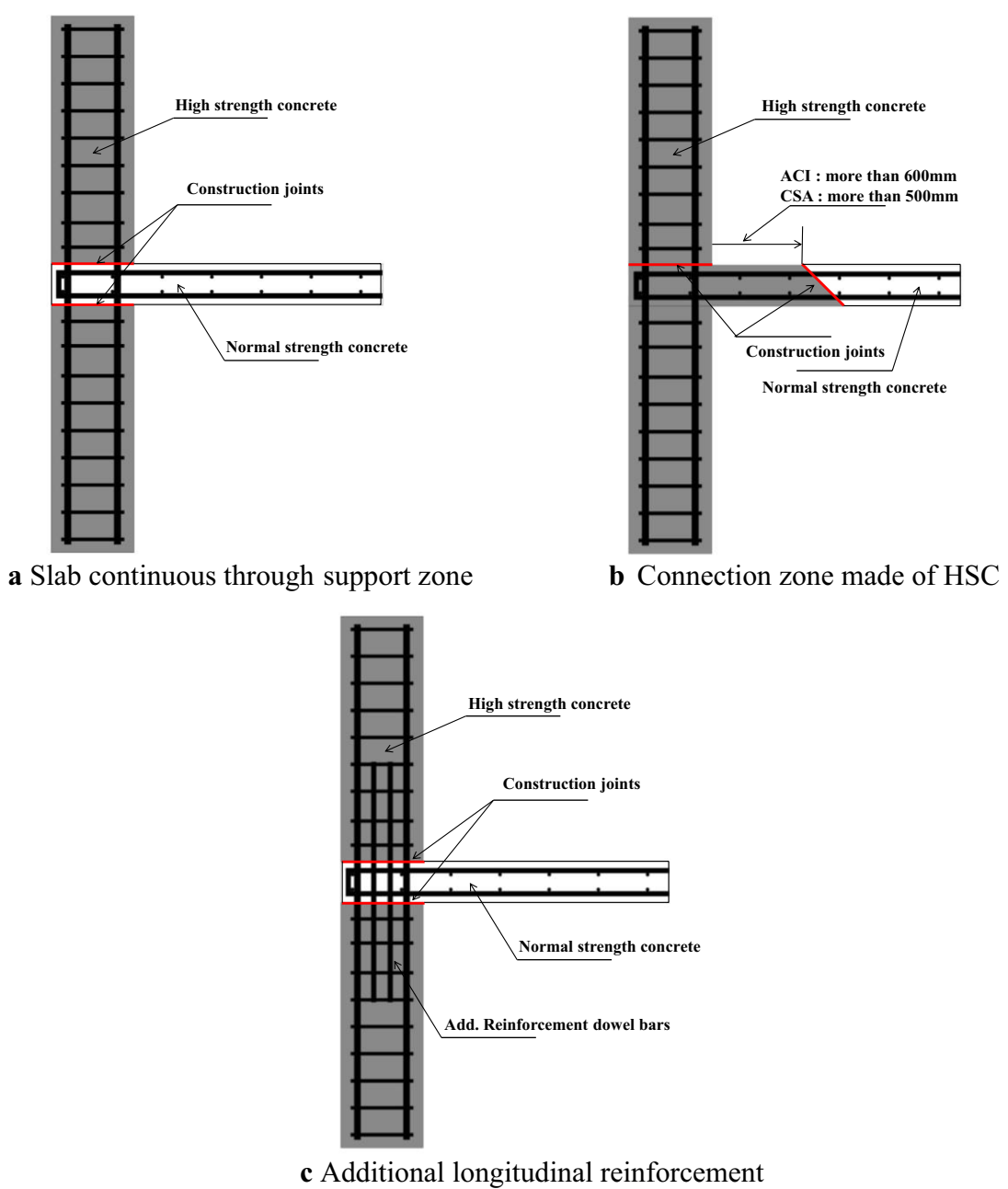


Fig. 1 Type of column-slab connection (Urban and Gołdyn 2015).

(hereinafter referred to as an exterior column), the column concrete strength (f'_{cc}) can be used as the effective compressive strength of the column (f'_{ce}) when the compressive strength of the column (f'_{cc}) does not exceed 1.4 times the slab compressive strength (f'_{cj}), whereas the compressive strength of the slab concrete (f'_{cj}) can be used as the effective compressive strength of the column (f'_{ce}) when the compressive strength of the column

(f'_{cc}) exceeds 1.4 times the slab compressive strength (f'_{cj}). The CSA A23.3-14 suggests that when the column concrete compressive strength (f'_{cc}) exceeds the slab concrete compressive strength (f'_{cj}), the column concrete should either be extended beyond the column face by a distance greater than 500 mm as shown in Fig. 1b, be reinforced with a vertical dowels or spirals as shown in Fig. 1c, or adopt the following effective compressive strength (f'_{ce}).

a. For interior columns

$$f'_{ce} = 1.05f'_{cj} + 0.25f'_{cc} \leq f'_{cc} \quad (1a)$$

b. For exterior columns

$$f'_{ce} = 1.4f'_{cj} \leq f'_{cc} \quad (1b)$$

c. For corner columns

$$f'_{ce} = f'_{cj} \quad (1c)$$

In attempts to estimate the effective concrete strength of HSC columns with intervening NSC slabs, many researchers have conducted a number of experimental studies (Lee and Mendis 2004; Gamble and Klinar 1991; Bianchini et al. 1960; Kayani 1992; Shu and Hawkins 1992; Ospina and Alexander 1998; McHarg et al. 2000; Shah et al. 2005). These studies have varied the number of sides of the column confined by slab, the compressive strength ratio of the column and slab (f'_{cc}/f'_{cj}), and the ratio of slab thickness to column section dimension (h/c). From the test results, they proposed empirical or semi-empirical models for estimating the effective compressive strength. However, the proposed models were developed solely based on the results of experimental research without any analytical research, and the equations of effective compressive strength presented in the current design codes (ACI 318-19; CSA A23.3-14) were also derived solely from the test results of the existing research. Therefore, a theoretical study is necessary to further elucidate the background of the effective compressive strength and load transfer mechanism between columns and slabs with different compressive strengths.

HSC columns and NSC slabs are subjected to the same compressive stress due to the axial load. However, the vertical strains of the column and slab are different, and the horizontal strains are different as well. As a result, tensile and compressive stresses occur in the column and the slab, respectively, in the orthogonal direction of the axial load. Choi et al. (2018) estimated the stresses induced by the orthogonal strains of columns and slabs, and theoretically proposed the effective compressive strengths of corner and exterior columns by deriving the vertical-horizontal stress interaction curve of the column and slab. The model proposed by Choi et al. (2018) provided analysis results that were very similar to the test results. However, it requires a complex iterative calculation process to estimate the stress demand curves of the column and slab as well as the failure criteria of the column and slab, which makes it difficult to be used as a design equation.

Therefore, this study sought to simplify the proposed model of Choi et al. (2018) and propose a design equation

for the effective compressive strengths of isolated, corner and exterior columns. This study does not include interior column, i.e., surrounded by beams or slabs on four sides. The study on interior columns will be carried out in the future using the theoretical approach of corner and exterior columns performed in this study. In this regard, the axial loading test was conducted on the isolated columns with no confinement of slabs. Then, the test results were compared with the effective compressive strength obtained from the proposed equation.

2 Detailed Model

When columns are subject to arbitrary compressive force (P_i), HSC columns and NSC slabs experience the same compressive stress (σ_i). By contrast, the vertical strains that occur in the HSC columns and NSC slabs vary, which in turn produces differences in the horizontal strain caused by the Poisson effect. However, since the interface between the HSC column and the NSC slab is synthesized, both the column and the slab are expected to exhibit the same horizontal strain. Due to this compatibility condition, the compressive stress in the horizontal direction is applied to the NSC slab in the vicinity of the column-slab interface, while the tensile stress in the horizontal direction occurs in the HSC column, indicating a mutually intervening stress status. As shown in Fig. 2, Choi et al. (2018) determined the effective compressive strength of the column based on the mechanism that first reaches the corresponding potential capacity among the multi-axial stress behavior curve (compression-tension-tension) occurring in the HSC column and the tri-axial compressive stress behavior curve occurring in the NSC slab. As shown in Fig. 2, the vertical axis represents the vertical compressive stress (σ_i) applied to the column and slab concrete while the horizontal axis represents the horizontal stress of the column and slab ($d\sigma_{cc0}$ and $d\sigma_{cj0}$) induced in interfacial concrete caused by the mutual interference between the column and slab. The curves indicated by straight lines are the vertical-horizontal stress interaction curves ($\sigma_{cc0,behavior}$ and $\sigma_{cj0,behavior}$) that occur in the slabs and columns subject to axial stresses, while the dotted lines are the failure criterion curves ($\sigma_{cc0,failure}$ and $\sigma_{cj0,failure}$) of the slabs and columns, respectively. Among the intersecting points of the stress interaction curves and the corresponding failure criterion curves, the smallest value is determined to be the effective compressive strength column (f'_{ce}) of the column.

In the study conducted by Choi et al. (2018), the tensile strain $d\varepsilon_{cc0}$ and tensile stress $d\sigma_{cc0}$ occurring in the column as well as the compressive strain $d\varepsilon_{cj0}$ and compressive stress $d\sigma_{cj0}$ occurring in the slab were calculated using the force equilibrium condition and strain

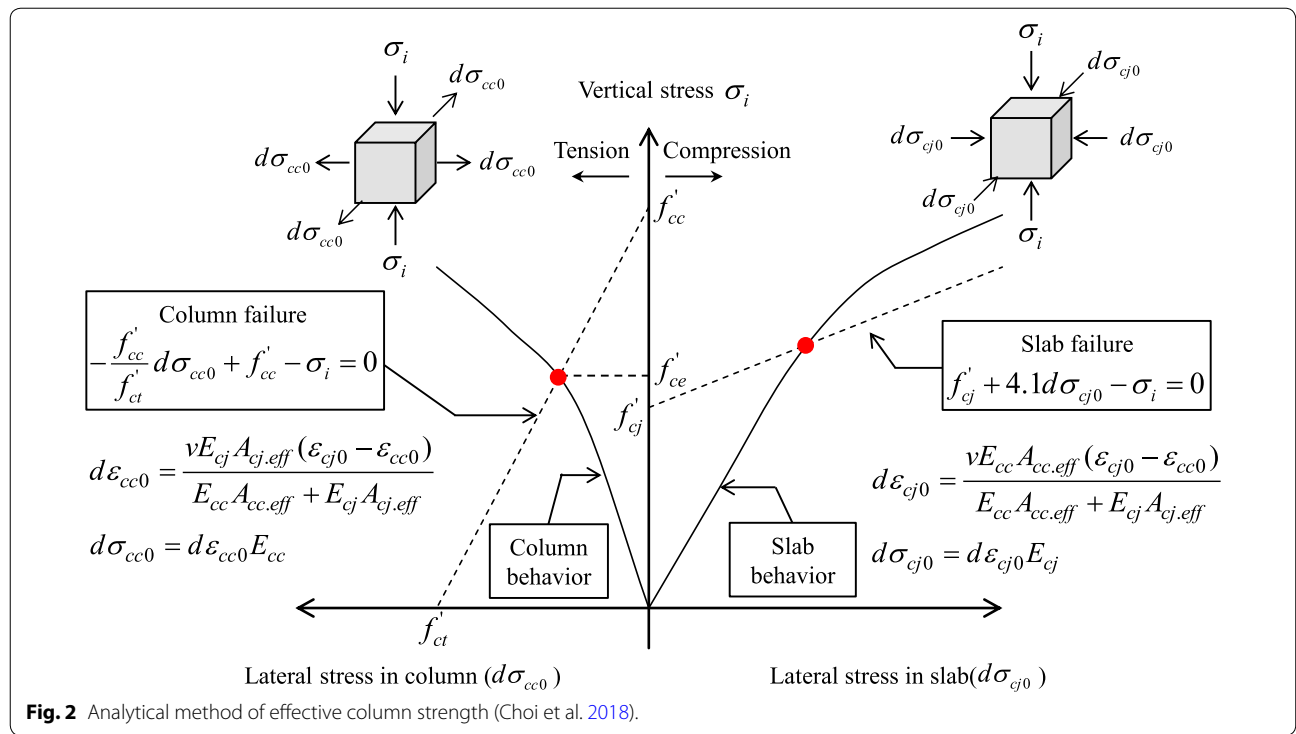


Fig. 2 Analytical method of effective column strength (Choi et al. 2018).

compatibility condition in the interference zone between the column and slab, as follows:

$$d\epsilon_{cc0} = \frac{vE_{cj}A_{cj,eff}(\epsilon_{cj0} - \epsilon_{cc0})}{E_{cc}A_{cc,eff} + E_{cj}A_{cj,eff}} \quad (2a)$$

$$d\sigma_{cc0} = \frac{vE_{cc}E_{cj}A_{cj,eff}(\epsilon_{cj0} - \epsilon_{cc0})}{E_{cc}A_{cc,eff} + E_{cj}A_{cj,eff}} \quad (2b)$$

$$d\epsilon_{cj0} = \frac{vE_{cc}A_{cc,eff}(\epsilon_{cj0} - \epsilon_{cc0})}{E_{cc}A_{cc,eff} + E_{cj}A_{cj,eff}} \quad (3a)$$

$$d\sigma_{cj0} = \frac{vE_{cc}E_{cj}A_{cc,eff}(\epsilon_{cj0} - \epsilon_{cc0})}{E_{cc}A_{cc,eff} + E_{cj}A_{cj,eff}} \quad (3b)$$

where v is Poisson's ratio of the concrete and ϵ_{cc0} and ϵ_{cj0} are the vertical compressive strains of the column and slab concrete, respectively. Further, E_{cc} and E_{cj} are the elastic modulus of the concrete for the column and slab, respectively. Finally, $A_{cc,eff}$ and $A_{cj,eff}$ are the effective interference area of the column and slab, respectively, and can be calculated as follows:

$$A_{cc,eff} = \frac{1}{6}c^2 \quad (4)$$

$$A_{cj,eff} = \frac{1}{6}c^2 \quad (\text{when, } c \leq 3h) \quad (5a)$$

$$A_{cj,eff} = \frac{1}{2}ch \quad (\text{when, } c > 3h) \quad (5b)$$

where c is column width and h is slab thickness. Based on the bi-axial strength failure envelope of concrete proposed by Kupfer et al. (1969) and the tri-axial compression test on the concrete cylinder specimens (Richart et al. 1928), the column and slab failure criteria ($\sigma_{cc0,failure}$ and $\sigma_{cj0,failure}$) were estimated using the following equations.

$$\sigma_{cc0,failure}(d\sigma_{cc0}, \sigma_i) = -\frac{f'_{cc}}{f'_{ct}} d\sigma_{cc0} + f'_{cc} - \sigma_i = 0 \quad (6a)$$

$$\sigma_{cj0,failure}(d\sigma_{cj0}, \sigma_i) = f'_{cj} + 4.1d\sigma_{cj0} - \sigma_i = 0 \quad (6b)$$

where f'_{ct} is the tensile strength of the column concrete, which was assumed to be $0.6\sqrt{f'_{cc}}$.

3 Simplified Model

Figure 3 shows the process of estimating the effective compressive strength of the column using a detailed model. When an axial load is applied to the column, a vertical stress (σ_i) is generated while moving point ① to point ②, and the potential capacity ($\sigma_{cc0,failure}$) of

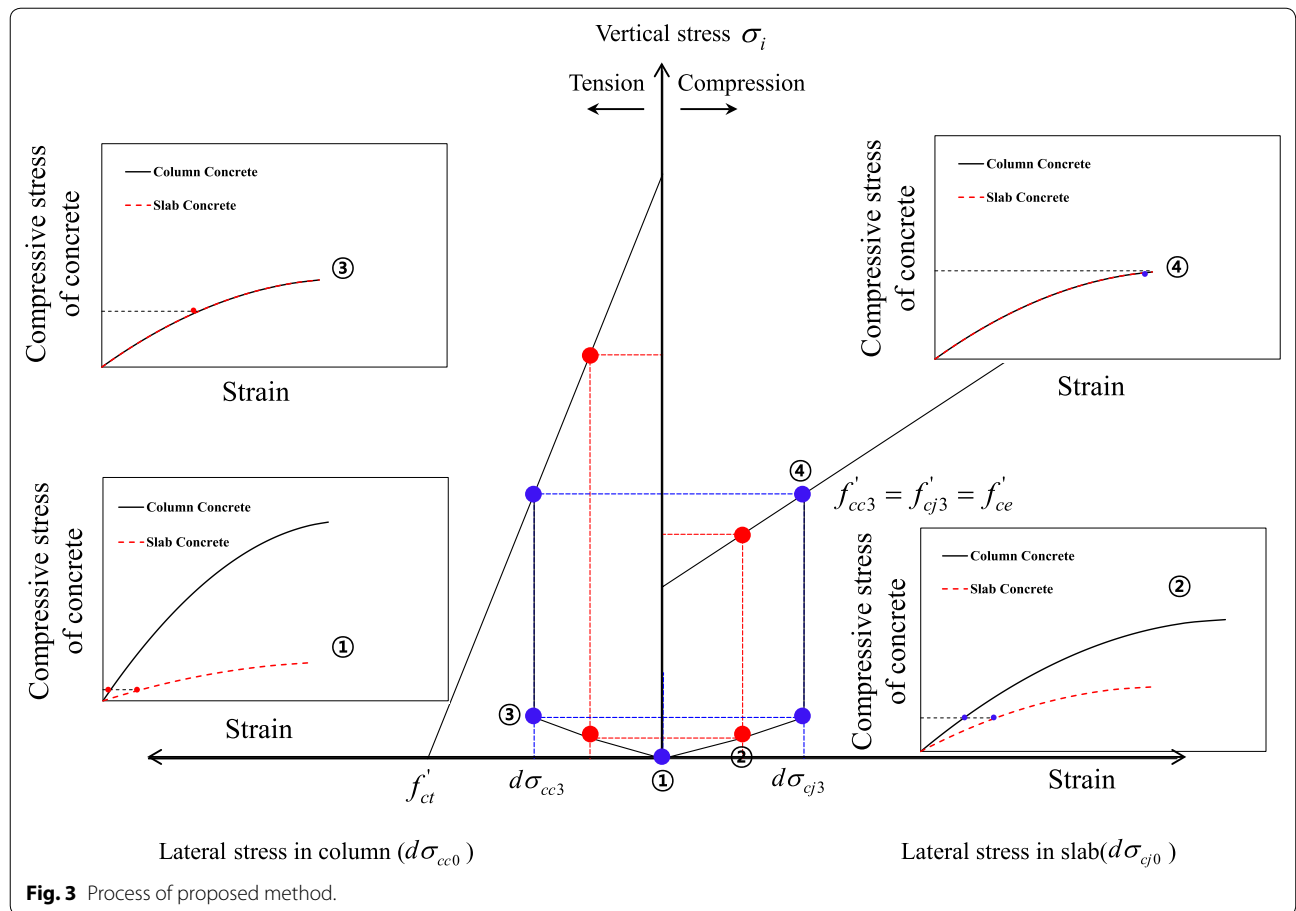


Fig. 3 Process of proposed method.

the column in the interference zone decreases while the potential capacity ($\sigma_{cj0,failure}$) of the slab increases due to the tensile stress generated in the column and the compressive stress generated in the slab. As a result, the stress-strain relationship between the column and slab concrete varies, and the difference in compressive strength between the column and slab concrete decreases. With increasing vertical stress, the strength difference between the column and slab concrete gradually decreases, and there exists a point at which the capacity of the column and slab concrete becomes equal, which is referred to as point ③. Meanwhile, if the stress behavior curves of the column or slab reach the failure criteria before reaching point ③, the lower value of the two is determined to be the effective compressive strength. If point ③ is successfully reached, no further confinement stress occurs, since the horizontal strain generated by the Poisson effect of the column and slab at the interface is the same. Therefore, in the column and slab concrete after point ③, only the vertical stress increases while the horizontal stress ceases to increase. Ultimately, the vertical stress at point ④ is determined to be the effective compressive strength of the column. The

effective compressive strength (f_{ce}') can be represented by the following equation through the assumption that behavior curves of column and slab do not reach the failure criteria before reaching point ③.

$$f_{ce}' = f_{cc}' \left(1 - \frac{d\sigma_{cc0}}{0.6\sqrt{f_{cc}'}} \right) = f_{cj} + 4.1d\sigma_{cj0} \quad (7)$$

The following relation can be derived from the force equilibrium condition in the column-slab interference zone.

$$d\sigma_{cc0}A_{cc,eff} - d\sigma_{cj0}A_{cj,eff} = 0 \quad (8)$$

The effective compressive strength can be calculated using Eqs. (7) and (8) without the need for iterative calculations. Equation (8) can be represented using the effective interference area of the column and slab as follows:

$$d\sigma_{cj0} = K \cdot d\sigma_{cc0} \quad (9)$$

where K is the effective interfacial area ratio of the column and slab ($A_{cc,eff}/A_{cj,eff}$) and can be calculated based

on the width of the column (c) and the thickness of the slab (h) as follows:

$$K = 1 \quad (\text{when, } c \leq 3h) \quad (10a)$$

$$K = \frac{A_{cc,eff}}{A_{cj,eff}} = \frac{c}{3h} \quad (\text{when, } c > 3h) \quad (10b)$$

From Eqs. (7) and (9), the following equation can be derived.

$$Q \cdot d\sigma_{cc0} = f'_{cc} - f'_{cj} \quad (11)$$

where Q is $4.1K + \sqrt{f'_{cc}}/0.6$. With (9) and (11) summarized, the effective compressive strength of the column can be estimated in a simple manner using the equation below.

$$f'_{ce} = f'_{cj} + 4.1 \frac{K}{Q} \left(f'_{cc} - f'_{cj} \right) \quad (12)$$

4 Experimental Research

Figure 4 and Table 1 show the detailed dimensions and material properties of the specimens. The width of the square column is 200 mm, the thickness of the joint is 100 mm, the height of both the upper and lower columns is 600 mm, and the total height of the entire column is 1300 mm. 4-D13 rebar with a yield strength of 419.2 MPa was used as the longitudinal reinforcement, while a D6 rebar with a yield strength of 435.6 MPa was used for the transverse reinforcement. The C1 specimen is a control specimen, and the lower column, joint, and upper column were placed using the same compressive strength concrete (51.18 MPa). The C2 to C5 specimens were installed in the following order in order to reflect the real construction process: lower column, joint, then upper column. For the C2 specimen, the compressive strengths of the column and joint were 47.76 and 35.51 MPa, respectively. The strength ratio of the column and joint was 1.35. According to the ACI 318-19, the effective compressive strength for the C2 specimen does not need to be considered, because the strength ratio of the column to the joint is less than 1.4, but the decreased load transfer performance of the column must be considered in accordance with the CSA A23.3-14. The column-joint compressive strength ratios of the C3 and C4 specimens were 1.44 and 1.40, respectively. In this case, the decreased load transfer performance should be considered in not only the CSA A23.3-14 but also the ACI 318-19. The C5 specimen has a joint thickness of 200 mm, while the ratio of the joint thickness to the column section dimension (h/c) is 1.0. The total height of the column is 1300 mm, like the other specimens, the height of both the upper and lower column is 550 mm, and the remaining details are the same as those of the C3 specimen. As shown in Fig. 5a, metal shoes were installed so as to avoid failure caused by stress concentration at the ends of the columns. As shown in Fig. 5b, in order to measure the deformation of the columns and slabs during the test, linear variable differential transformers (LVDTs) were

Table 1 Specimens details.

	c (mm)	h (mm)	f'_{cc} (MPa)	f'_{cj} (MPa)	f'_{cc}/f'_{cj}	A_s (mm 2)	f_y (MPa)
C1	200	100	51.18	51.18	1.00	506.8	419.2
C2	200	100	47.76	35.51	1.35	506.8	419.2
C3	200	100	51.18	35.51	1.44	506.8	419.2
C4	200	100	49.77	35.51	1.40	506.8	419.2
C5	200	200	51.18	35.51	1.44	506.8	419.2

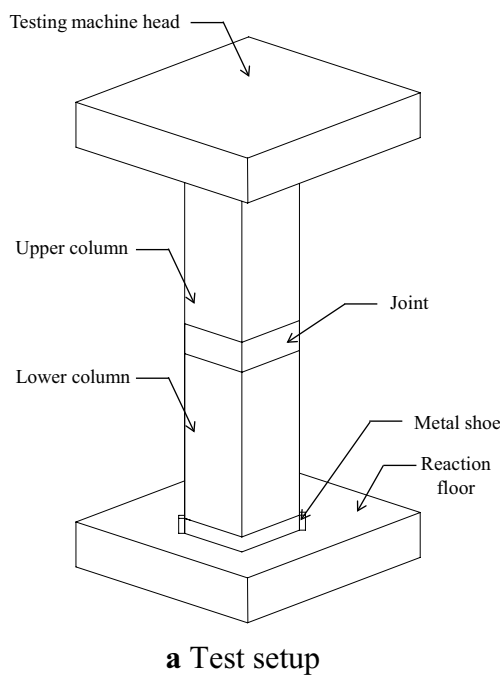


Fig. 5 Test setup.

installed on the upper and lower columns and slabs. The load was applied using a universal testing machine with a maximum compressive capacity of 5,000kN under displacement control.

4.1 Test Results and Discussion

Table 2 summarizes the test results of the specimens. According to the ACI 318-19, the axial force (P_o) of the column without eccentricity is given as follows.

Table 2 Summary of test and analysis results.

Specimens	f'_{cc} / f'_{cj}	P_{test} (kN)	$f'_{ce,test}$ (MPa)	$f'_{ce,pro}$ (MPa)	$f'_{ce,test} / f'_{ce,pro}$
C1	1.00	1928.0	51.10	—	—
C2	1.35	1512.6	38.73	38.73	1.00
C3	1.44	1786.7	46.90	39.52	1.19
C4	1.40	1725.0	45.06	39.20	1.15
C5	1.44	1422.6	36.05	39.52	0.91
Average					1.06
SD					0.13
COV					0.12

$$P_0 = \alpha f'_c (A_g - A_s) + f_y A_s \quad (13)$$

where α is 0.85 in ACI 318-19 and 0.85–0.0015 f'_c in CSA A23.3-14; f'_c is the compressive strength of the concrete; A_g is the gross sectional area of the column; and A_s and f_y are the sectional area and yield strength of the longitudinal reinforcement in the column, respectively. In this study, the effective compressive strength of the test specimen ($f'_{ce,test}$) was calculated using the maximum axial force of the column (P_{test}) according to the test measurements and Eq (13), as follows:

$$f'_{ce,test} = \frac{P_{test} - f_y A_s}{\alpha (A_g - A_s)} \quad (14)$$

Figure 6 shows the axial load–axial strain responses of the test specimens. The axial strain of the specimen was calculated by dividing the deformation of the entire column measured from the LVDTs by the total length of the column. In all of the specimens, the strains at the maximum load were between 0.002 and 0.003, and most of them were failed in a brittle manner after reaching the

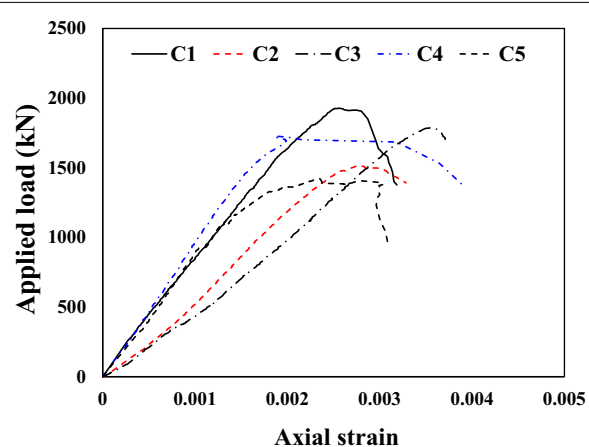


Fig. 6 Applied load–axial strain relationship.

maximum axial load. The maximum axial load of the C1 specimen with the same compressive strength of the column and joint was found to be 1928 kN, and the effective compressive strength calculated using Eq. (14) was 51.1 MPa, which was almost equal to the compressive strength of the cylinder specimen. For the C2 specimen with a column to joint strength ratio of 1.35, it is not necessary to use the effective compressive strength based on the ACI 318-19. However, the effective compressive strength of the C2 specimen derived from the test was 38.73 MPa, which indicates about a 19% reduction in compressive strength compared to the compressive strength of the upper column of 47.76 MPa. The maximum load of the C3 specimen (column-joint strength ratio 1.44) was 1786.7 kN and the effective compressive strength was 46.9 MPa, while the effective compressive strength of the C3 specimen calculated based on the ACI 318-19 was 35.51 MPa. The C2 and C3 specimens have the same joint concrete strength, and the column concrete strength of the C3 specimen is 51.18 MPa, which is higher than that of the C2 specimen (47.76 MPa). According to the ACI 318-19, however, the effective compressive strength of C3 specimen is smaller than C2 specimen because the ACI 318-19 code specifies that the effective strength equals to the concrete strength of the slab when the critical strength ratio of the column and joint exceeds 1.4, which is the case of C3 specimen. The maximum load of the C4 specimen was 1725.0 kN and the effective compressive strength was 45.06 MPa, which was reduced by about 9% compared to the compressive strength of the upper column (49.77 MPa). The maximum load of the C5 specimen was 1422.6 kN and the effective compressive strength was 36.05 MPa. For the C5 specimen, only the thickness of the joint increased in comparison with the C3 specimen, and the effective compressive strength was reduced by about 23% when compared to the C3 specimen (46.9 MPa), thus demonstrating a very notable difference.

Figure 7 shows the crack patterns at compression failure for each test specimen. Cracks hardly occurred until the maximum load was reached, which means that most cracks occurred immediately after reaching the maximum load. In all specimens, more cracks occurred in the upper column and joint than in the lower column. In addition, in the C3, C4, and C5 specimens, in which the strength ratio of column to joint or joint width was large, more damage occurred to the joint.

4.2 Verification of Proposed Model

In order to verify the proposed model, the test results from a total of seven studies were collected (Lee and Mendis 2004; Gamble and Klinar 1991; Bianchini et al. 1960; Shu and Hawkins 1992; McHarg et al. 2000; Shah

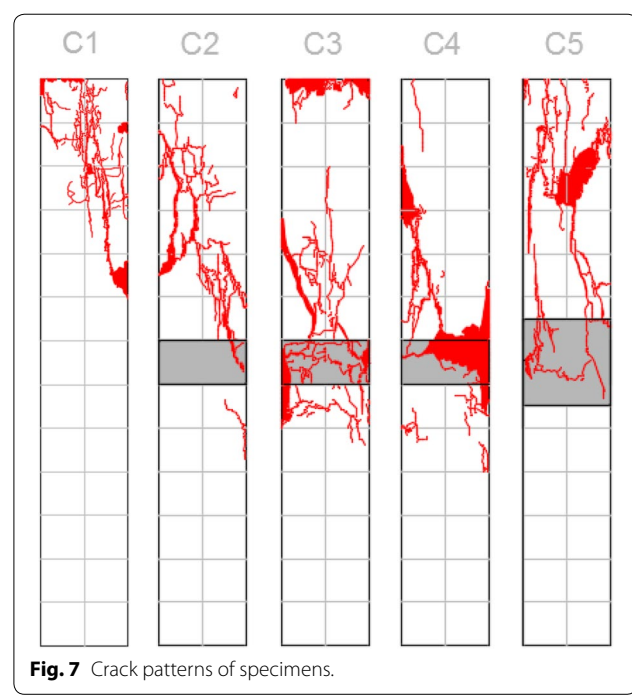


Fig. 7 Crack patterns of specimens.

et al. 2005; Lee et al. 2007) and the collected test results are summarized in Table 3 along with the experimental results derived from this study. Figure 8 shows a comparison of the test results and analysis results through the effective compressive strength equation presented in ACI 318-19 and CSA A23.3-14 as well as the analysis model proposed in this study. The horizontal axis represents the effective compressive strengths of the test specimens ($f'_{ce,test}$) calculated using Eq. (14), and the vertical axis represents the analysis results (f'_{ce}) estimated through the code equation or the proposed model. The results of the calculations through ACI 318-19 showed that the average (AVG) ratio of the test results to the analysis results ($f'_{ce,test}/f'_{ce}$) was 1.659, exhibiting a very conservative result, and the coefficient of variation (COV) was 0.488, leading to a large deviation of $f'_{ce,test}/f'_{ce}$. The effective compressive strength presented in the CSA A23.3-14 also found to provide fairly conservative analysis results, as the AVG and the COV were respectively estimated to be 1.762 and 0.478. By contrast, for the proposed model, the AVG and the COV were found to be 1.200 and 0.211, respectively. Therefore, it was confirmed that the proposed model not only conservatively predicted the effective compressive strengths of the test specimens, but also exhibited superior analytical accuracy over the current design codes. In this sense, the proposed model is expected to have a high utilization value in practical design.

Table 3 Summary of corner and exterior column test specimens.

Researcher	Specimen ID	f'_{cc} (MPa)	f'_{cj} (MPa)	$f'_{ce,test}$ (MPa)	Researcher	Specimen ID	f'_{cc} (MPa)	f'_{cj} (MPa)	$f'_{ce,test}$ (MPa)
Shu and Hawkins	A	48.6	35.0	41.2	Bianchini et al.	E-4	48.5	18.0	33.8
	B	48.6	35.0	43.6		E-5	48.5	18.0	37.8
	C	48.6	35.0	41.2		E-6	48.5	18.0	39.8
	D	46.6	34.9	40.5		S75S3.0	36.7	15.0	19.0
	E	46.6	34.9	37.3		S60S2.4	35.5	13.5	17.0
	FT	47.6	31.4	34.1		S50S2.0	35.9	15.0	19.6
	G	47.6	31.4	30.5		S37S1.5	20.8	13.5	17.9
	H	50.8	23.6	23.2		S90C3.0	52.0	17.0	23.1
	I	50.8	23.6	31.0		S75C3.0	51.2	18.5	25.2
	J	50.8	23.6	39.5		S60C3.0	37.1	8.8	17.5
	K	48.8	30.9	37.5		S60C2.0	45.7	24.8	27.3
	A-1	40.8	39.2	35.0		S50C2.0	38.2	17.6	21.3
	A-2	40.8	39.2	34.2		S40C2.0	24.2	10.4	16.6
	A-3	40.8	39.2	34.7		S45C1.5	27.5	18.8	21.1
	A-4	40.8	39.2	33.5		S37C1.5	22.5	15.9	18.5
	A-5	40.8	39.2	35.1		S30C1.5	16.5	10.5	12.8
	A-6	40.8	39.2	34.3		S90E3.0	52.5	16.8	28.3
	B-1	45.4	21.1	16.6		S75E3.0	46.9	16.4	26.2
	B-2	45.4	21.1	20.0		S60E3.0	35.8	11.9	20.8
	B-3	45.4	21.1	26.4		S60E2.0	45.1	23.9	29.0
	B-4	45.4	21.1	32.0		S50E2.0	35.3	16.2	21.5
	B-5	45.4	21.1	35.6		S40E2.0	23.2	9.6	16.4
	B-6	45.4	21.1	35.9		S45E1.5	23.8	17.7	21.3
	C-1	45.8	23.8	23.9	Lee and Mendis	S37E1.5	20.8	13.7	18.6
	C-2	45.8	23.8	24.9		S30E1.5	15.8	10.1	15.4
	C-3	45.8	23.8	31.7		SC1	80.6	17.5	33.7
	C-4	45.8	23.8	35.4		SC2	77.4	20.7	32.1
	C-5	45.8	23.8	37.0		SC3	83.9	28.2	31.7
	C-6	45.8	23.8	37.6		A	86.2	28.3	43.9
	D-1	38.6	6.9	8.6	Gamble and Klinar	B	86.9	25.5	42.1
	D-2	38.6	6.9	10.2		E	90.3	45.5	57.9
	D-3	38.6	6.9	15.8		FT	97.9	15.9	38.6
	D-4	38.6	6.9	24.6		I	92.4	30.3	57.9
	D-5	38.6	6.9	27.8		J	79.3	36.5	61.4
	D-6	38.6	6.9	36.0		CN	80.7	30	43.8
	E-1	48.5	18.0	15.5	McHarg et al.	C2	47.8	35.5	38.7
	E-2	48.5	18.0	17.7		C3	51.2	35.5	46.9
	E-3	48.5	18.0	24.7		C4	49.8	35.5	45.1
Shah et al.	SCSB-1	84	29	42.3		C5	51.2	35.5	36.1
Lee et al.	NC	88.33	46.89	53.3					

5 Conclusion

In this study, the compressive strengths of HSC columns with intervening NSC slabs were investigated, and a simplified equation for estimating the effective compressive strength of the column was proposed, based on the analytical research. In addition, the proposed equation was

verified by comparing with the compression test results obtained from this study and collected from literature. The following conclusions were derived from this study.

1. In the ACI 318-19, it is understood that there is no decrease in the compressive strength of the column

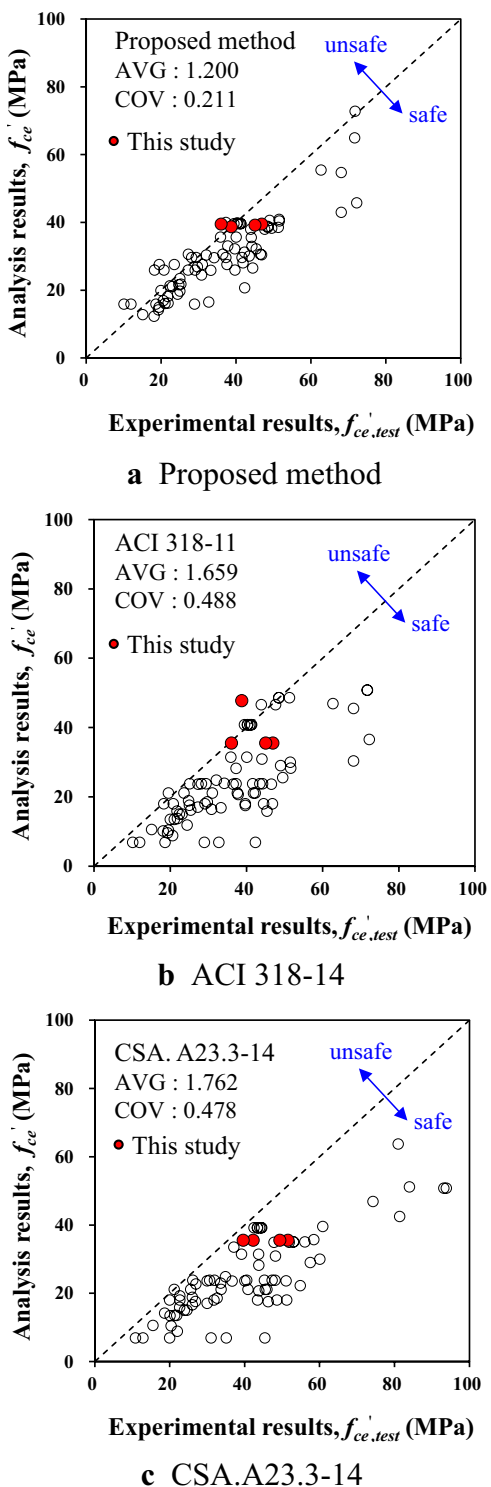


Fig. 8 Comparisons of test and analysis results.

when the compressive strength ratio of the column and slab concrete (f'_{cc}/f'_{cj}) is less than 1.4. However, the test results of isolated columns showed a reduction in the strengths of the columns in the cases of $f'_{cc}/f'_{cj} < 1.4$. Therefore, it can be concluded that the effective compressive strength provision presented in the ACI 318-19 demonstrates some unreasonable aspect; further study is still required though.

2. In this study, a simplified equation for effective compressive strengths was derived by applying the failure criteria of the column and slab, as well as the force equilibrium condition in the column-slab interference zone. The proposed equation was proven to be capable of estimating the effective compressive strengths without the need for a complex iterative calculation process.
3. According to the results of analysis on the test specimens obtained using the proposed model, the proposed model not only provided conservative results on the effective compressive strengths of the test specimens, but also evaluated them with a high accuracy compared to the current design codes (ACI 318-19, CSA A23.3-14). Therefore, it is expected that the proposed model may prove very useful in terms of practical design.

Abbreviations

f'_{ce} : Effective compressive strength; f'_{cc} : Concrete compressive strength of the column; f'_{cj} : Concrete compressive strength of the slab; σ_{cc0} : Horizontal stress of the column; σ_{cj0} : Horizontal stress of the slab; ϵ_{cc0} : Tensile strain occurring in the column; σ_{cc0} : Tensile stress occurring in the column; ϵ_{cj0} : Compressive strain occurring in the slab; σ_{cj0} : Compressive stress occurring in the slab; v : Poisson's ratio of the concrete; ϵ_{cc0} : Vertical compressive strains of the column; ϵ_{cj0} : Vertical compressive strains of the slab; E_{cc} : Elastic modulus of the concrete for the column; E_{cj} : Elastic modulus of the concrete for the slab; $A_{cc,eff}$: Effective interference area of the column; $A_{cj,eff}$: Effective interference area of the slab; c : Column width; h : Slab thickness; f'_c : Tensile strength of the column concrete; A_g : Gross sectional area of the column; A_s : Sectional area of the longitudinal reinforcement in the column; f_y : Yield strength of the longitudinal reinforcement in the column.

Acknowledgements

This research was supported by Basic Science Research Program through the National Research Foundation of Korea (NRF) funded by the Ministry of Education. (No. 2018R1A4A1025953).

Authors' contributions

Investigation, HCC and JHK; Supervision, KSK; Validation, JHH and SJH; Writing-original draft, SHC; Writing-review and editing, KSK.

Author's information

Seung-Ho Choi, Ph.D., Postdoctoral Fellow, Department of Architectural Engineering, University of Seoul, 163 Siripdaero, Dongdaemun-gu, Seoul 02504, Republic of Korea.

Jin-Ha Hwang, Ph.D., Researcher, Jeonnam and Jeju Branch, Korea Conformity Laboratories, 137, Yeosusan-dan-ro, Yeosu-si, Jeollanam-do 59631, Republic of Korea.

Sun-Jin Han, Ph.D., Postdoctoral Fellow, Department of Architectural Engineering, University of Seoul, 163 Siripdaero, Dongdaemun-gu, Seoul 02504, Republic of Korea.

Hae Chang Cho, Ph.D., Senior Researcher, Technology Center, Dream Structural Engineers, 1004, 10, Dongtan-daero 21-gil, Hwaseong-si, Gyeonggi-do, Republic of Korea.

Jae Hyun Kim, Ph.D. Candidate, Department of Architectural Engineering, University of Seoul, 163 Siripdaero, Dongdaemun-gu, Seoul 02504, Republic of Korea.

Kang Su Kim, Ph.D., Professor, Department of Architectural Engineering, University of Seoul, 163 Siripdaero, Dongdaemun-gu, Seoul 02504, Republic of Korea.

Funding

National Research Foundation of Korea, NRF-No. 2018R1A4A1025953.

Availability of data and materials

Not applicable.

Competing interests

The authors declare that they have no competing interests.

Author details

¹ Department of Architectural Engineering, University of Seoul, 163 Siripdaero, Dongdaemun-gu, Seoul 02504, Republic of Korea. ² Jeonnam and Jeju Branch, Korea Conformity Laboratories, 137, Yeosusan-dan-ro, Yeosu-si, Jeollanam-do 59631, Republic of Korea. ³ Technology Center, Dream Structural Engineers, 1004, 10, Dongtan-daero 21-gil, Hwaseong-si, Gyeonggi-do, Republic of Korea.

Received: 2 January 2020 Accepted: 16 May 2020

Published online: 24 July 2020

References

ACI Committee 318. (2019). *Building code requirements for structural concrete and commentary (ACI 318-19)*. Farmington Hills: American Concrete Institute.

- Bianchini, A. C., Woods, R. E., & Kesler, C. E. (1960). Effect of floor concrete strength on column strength. *ACI Journal Proceedings*, 56(5), 1149–1170.
- Canadian Standards Association Design of Concrete Structure (CSA A23.3-14), Canadian Standards Association, Mississauga, Ontario.
- Choi, S. H., Lee, D. H., Hwang, J. H., Oh, J. Y., Kim, K. S., & Kim, S. H. (2018). Effective compressive strength of corner and exterior concrete columns intersected by slabs with different compressive strengths. *Archives of Civil and Mechanical Engineering*, 18(3), 731–741.
- Gamble, W. L., & Klinar, J. D. (1991). Tests of high-strength concrete columns with intervening floor slabs. *ASCE Journal of Structural Engineering*, 117(5), 1462–1476.
- Kayani, M.K. (1992) Load transfer from high-strength concrete columns through lower strength concrete slabs, Ph.D. thesis, Department of Civil Engineering, University of Illinois, Urbana-Champaign, Ill.
- Kupfer, H., Hilsdorf, H. K., & Rusch, H. (1969). Behavior of concrete under biaxial stresses. *ACI Structural Journal*, 66(8), 656–666.
- Lee, S. C., & Mendis, P. (2004). Behavior of high-strength concrete corner columns intersected by weaker slabs with different thicknesses. *ACI Structural Journal*, 101(1), 11–18.
- Lee, J. H., Yang, J. M., Lee, S. H., & Yoon, Y. S. (2007). Improved transmission of UHSC column loads by puddling of fiber reinforced UHSC. *Journal of Korea Concrete Institution*, 19(2), 209–216. (in Korean).
- McHarg, P. J., Cook, W. D., Mitchell, D., & Yoon, Y. S. (2000). Improved transmission of high-strength concrete column loads through normal strength concrete slabs. *ACI Structural Journal*, 97(1), 149–157.
- Ospina, C. E., & Alexander, S. D. B. (1998). Transmission of interior concrete column loads through floors. *ASCE Journal of Structural Engineering*, 124(6), 602–610.
- Richart, F.E., Brandtzaeg, A., Brown, R.L. (1928) A study of the failure of concrete under combined compressive stresses, Bulletin NO. 185, University of Illinois.
- Shah, A. A., Dietz, J., Tue, N. V., & Koenig, G. (2005). Experimental investigation of column-slab joints. *ACI Structural Journal*, 102(1), 103–113.
- Shu, C. C., & Hawkins, N. M. (1992). Behavior of columns continuous through concrete floors. *ACI Structural Journal*, 89(4), 405–414.
- Urban, T. S., & Goldyn, M. M. (2015). Behaviour of eccentrically loaded high-strength concrete columns intersected by lower-strength concrete slabs. *Structural Concrete*, 16(4), 480–495.

Publisher's Note

Springer Nature remains neutral with regard to jurisdictional claims in published maps and institutional affiliations.

Submit your manuscript to a SpringerOpen® journal and benefit from:

- Convenient online submission
- Rigorous peer review
- Open access: articles freely available online
- High visibility within the field
- Retaining the copyright to your article

Submit your next manuscript at ► springeropen.com